https://doi.org/10.5194/egusphere-2024-4021
Preprint. Discussion started: 9 January 2025

Survival strategies of Antarctic vegetation during extensive glacial expansion across the Oligocene/Miocene Transition

Bella J. Duncan[1], Robert McKay[1], Richard Levy[1,2], Joseph G. Prebble[2], Timothy Naish[1], Osamu Seki[3], Christoph Kraus[1], Heiko Moossen[4,5], G. Todd Ventura[2,6], Denise K. Kulhanek[7], James Bendle[4]

[1] Antarctic Research Centre, Victoria University of Wellington, Wellington, 6140, New Zealand
[2] Geological and Nuclear Sciences, P.O. Box 30-368, Lower Hutt 5040, New Zealand
[3] Institute of Low Temperature Science, Hokkaido University, N19W8, Kita-ku, Sapporo, Hokkaido 060-0819, Japan
[4]School of Geography, Earth and Environmental Sciences, University of Birmingham, Edgbaston, Birmingham, B15 2TT, UK
[5] Present address: Max Planck Institute for Biogeochemistry, P.O. Box 10 01 64, 07701 Jena, Germany
[6] Present address: Department of Geology, Saint Mary's University, 923 Robie Street, Halifax, Nova Scotia, B3H 3C3, Canada
[7]Institute of Geosciences, Christian-Albrechts-University of Kiel, 24118, Kiel, Germany

Correspondence to: Bella J. Duncan (Bella.Duncan@vuw.ac.nz)

Abstract. Antarctica's terrestrial ecosystems are at risk from a rapidly changing climate. Investigating how Antarctica's vascular plants responded to major climatic variations in the geological past, especially under atmospheric CO_2 values similar to modern and future projections, may provide insight into how organisms could migrate across the continent as conditions change. Here, we investigate vegetation trends across the Oligocene/Miocene Transition (OMT, ~23 Myr), one of the largest transient glaciations of the Cenozoic. Despite extensive ice sheet expansion, Antarctic vegetation survived throughout this glacial episode. We use compound specific isotope trends ($\delta^{13}C$ and $\delta^{2}H$) of plant waxes in an Antarctic proximal sediment core from the Ross Sea (Deep Sea Drilling Project site 270) to investigate the response and survival mechanisms of Antarctic vegetation during this event. We detect the first observation of a marked negative *n*-alkane $\delta^{13}C$ excursion over the OMT, coupled with a shift to more positive *n*-alkane $\delta^{2}H$. We interpret this as plants sacrificing water use efficiency to maintain photosynthesis and carbon uptake during increasing glacial conditions, as atmospheric CO_2 decreased and orbital configurations favoured shorter, colder growing seasons with lower light intensity. We consider further drivers of these isotopic trends to be enhanced aridity, and a shift to a stunted, low elevation vegetation. These findings establish the adaptability of ancient Antarctic vegetation under atmospheric CO_2 conditions comparable to modern, and mechanisms that allowed vegetation to keep a foothold on the continent despite prolonged hostile conditions.

1 Introduction

The modern Antarctic terrestrial ecosystem is limited to two native species of vascular plants, which occupy a narrow ecological niche on the Antarctic Peninsula (Colesie et al., 2023). A more diverse magellanic subpolar forest-tundra-type flora was widespread across Antarctica for much of the past 34 million years (e.g. Ashworth and Cantrill, 2004; Prebble et al., 2006;

https://doi.org/10.5194/egusphere-2024-4021
Preprint. Discussion started: 9 January 2025

Lewis et al., 2008; Warny et al., 2009). The timing of the demise of vascular plants from the continent is long debated but inferred to have occurred sometime between the late Miocene and Pliocene (~14 and 3 Ma) (Lewis et al., 2008; Fielding et al., 2012; Barrett et al., 2013; Wei et al., 2014). In the lead up to this eventual disappearance of widespread vegetation, intervals of large glacial expansion pushed Antarctic plants to the brink of their habitable zone.

The Oligocene/Miocene Transition (OMT) is marked by the transient Mi-1 glaciation at 23.03 Ma (Zachos et al., 1997; Naish et al., 2001). The Mi-1 event is represented by a positive benthic foraminiferal oxygen isotope excursion of ~0.6-1‰ over a 200-300 kyr interval. This large shift was caused in part by major expansion of the Antarctic Ice Sheets (AIS) from smaller-than-present terrestrial-based ice sheets to an AIS up to 25% greater in volume than present day (Zachos et al., 2001; Pekar and DeConto, 2006; Beddow et al., 2016). The Mi-1 glaciation arose from multiple drivers. Proxies indicate a drop in atmospheric CO_2 from ~500 ppm during the early Oligocene to preindustrial values during Mi-1 (CenCO2PIP, 2023). Proximal Antarctic cores also show cooling surface ocean temperatures in the Ross Sea and offshore Wilkes Land from ~24.5 Ma (Duncan et al., 2022). The Mi-1 glaciation is associated with a low in 400-kyr eccentricity (a more circular orbit) and a node in 1.2 Myr obliquity (low axial tilt) that resulted in an extended period of low seasonality and cooler summer temperatures, conditions favouring polar ice growth (Zachos et al., 2001; Pälike et al., 2006).

Here, we use plant wax compound-specific isotopes ($\delta^{13}C$ and $\delta^{2}H$) from a proximal Antarctic drill core to investigate how Antarctic vegetation responded to, and survived through, an extensive glacial period 23 million years ago. Deep Sea Drilling Project Site 270 (DSDP 270) comprises a sedimentary sequence that records advance and retreat of the AIS over the late Oligocene to early Miocene (Kulhanek et al., 2019; Olivetti et al., 2023). Importantly, environmental proxies gleaned from the sequence offer a means to examine changes in Antarctic vegetation through the Mi-1 event. DSDP 270 was drilled on the continental shelf in the Eastern Basin of the central Ross Sea in 1973 (77°26.48'S, 178°30.19'W), as part of DSDP Leg 28 (Fig. 1, The Shipboard Scientific Party, 1975). Seismic studies and models suggest that the bathymetry of the Ross Sea embayment was significantly shallower during the deposition of the sediments at DSDP 270, with basement highs and/or islands separated by deep basins (De Santis et al., 1999; Paxman et al., 2019). The stratigraphy of DSDP 270 is characterised by fluctuating ice-distal (mudstone) to ice-proximal (diamictite) sediments, recording the variable proximity of glacial ice to the core site (Kulhanek et al., 2019). In this study we examine compound specific isotopes of high molecular weight *n*-alkanes obtained from the core. These compounds come from plant waxes that were transported to the core site by wind, ocean currents and glacio-fluvial processes from vegetated areas onshore the Antarctic mainland and/or islands.

https://doi.org/10.5194/egusphere-2024-4021
Preprint. Discussion started: 9 January 2025

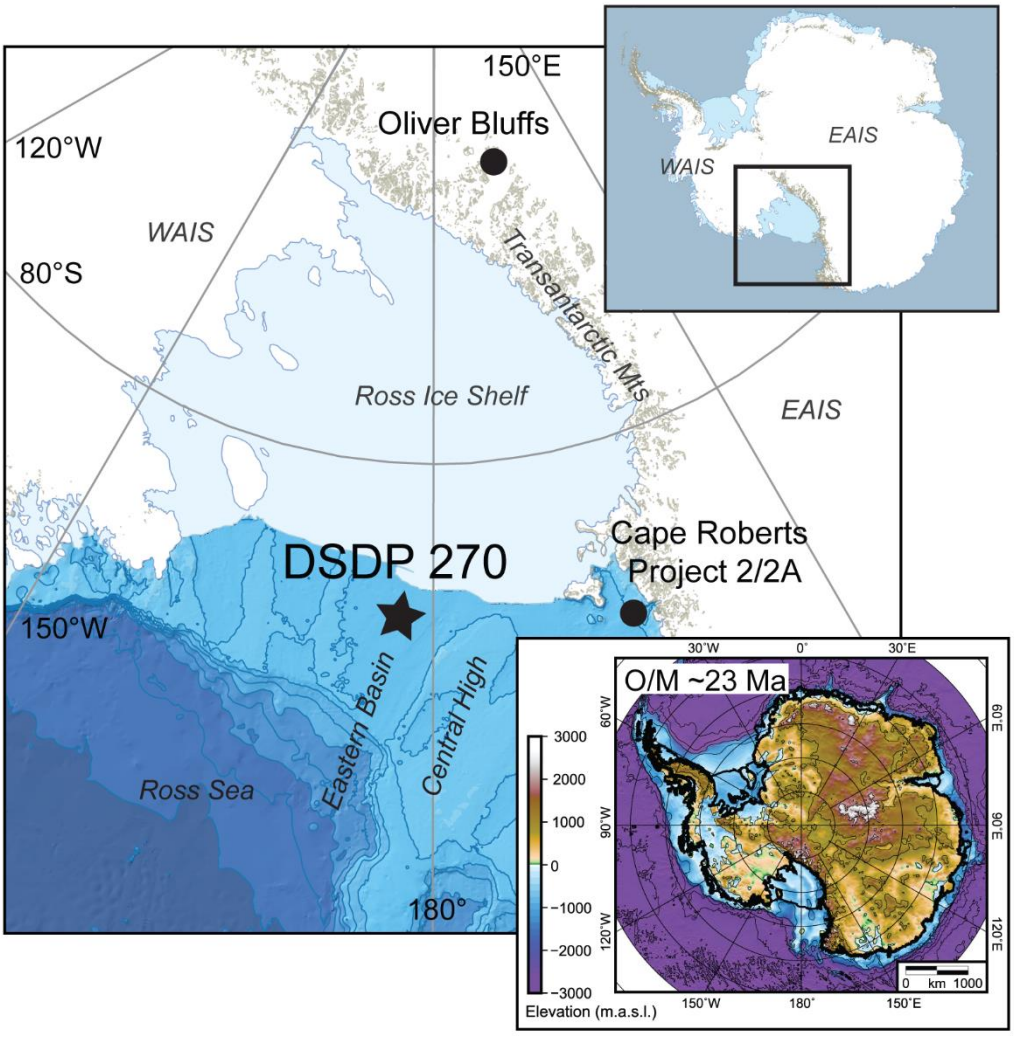

Figure 1: Location of DSDP 270 and other sites referred to in this study. WAIS: West Antarctic Ice Sheet, EAIS: East Antarctic Ice Sheet. Insert shows the reconstructed topography of Antarctica at the Oligocene/Miocene boundary[20], under a Creative Commons license CC BY. Base map from Quantarctica GIS package, Norwegian Polar Institute.

4. Methods

4.1. Lipid Biomarkers

Samples from DSDP 270 were obtained from the IODP Gulf Coast Repository at Texas A&M University and from archive samples held at GNS Science, New Zealand. Unless already desiccated, samples were freeze dried for 48 h prior to processing. All samples were homogenised to a powder using a Retsch 200 mixer mill. Organic geochemical work-up was performed in the Birmingham Molecular Climatology Laboratory (BMC), University of Birmingham. Lipids were extracted from ~10-15 g of homogenised sediment by ultrasonic extraction using 3:1 dichloromethane (DCM):methanol (MeOH) solution. The total

https://doi.org/10.5194/egusphere-2024-4021
Preprint. Discussion started: 9 January 2025

solvent extract was fractionated by silica gel chromatography, using *n*-hexane to isolate the aliphatic saturated and unsaturated hydrocarbons (e.g. *n*-alkanes). Procedural blanks were also analysed to ensure the absence of laboratory contaminants. *n*-Alkanes were identified and quantified using an Agilent 7890B series gas chromatograph (GC), equipped with a 7639ALS autosampler, a BP5-MS column (SGE Analytical Science, 60m × 0.32mm × 0.25µm) and an flame ionisation detector (FID), using hydrogen (H_2) as a carrier gas. The GC oven was programmed using a multi-ramp with a starting temperature of 70°C maintained for 1 min, followed by a 30°Cmin^{-1} ramp to 120°C, and a 30°Cmin^{-1} ramp to 320°C, which was held constant for 20 min. GC-Mass spectrometry (GC-MS) was performed using an Agilent 7890B GC, coupled to an Agilent 5977A Mass Selective Detector (MSD). The same capillary column and temperature program was used throughout the analyses for consistent compound separation. Helium (He) was used as a carrier gas. Samples were bracketed with an external standard containing known abundances of certain *n*-alkanes to allow identification and quantification of *n*-alkanes (average standard deviation of ± 7.6 %). *n*-Alkane peaks were integrated in Agilent OpenLAB Data Analysis Version A.01.01 - Build 1.93.0.

4.2. Compound specific isotopes

Carbon and hydrogen stable isotopes of *n*-alkanes *n*-C_{23} – *n*-C_{31} were analysed in the Organic Geochemistry Unit, University of Bristol. The $\delta^{13}C$ values were determined using an Isoprime 100 instrument interfaced via a GC5 interface to an Agilent 7890A GC with a split/splitless injector operating in splitless mode (splitless time of 2 min). Using helium as a carrier gas, 1µl of sample was injected on to a Restek column (Rtx-1 50m × 0.32mm × 0.17µm) and analysed with the temperature was held at 40 °C for 1 min, then increased to 300 °C at a rate of 10°Cmin^{-1} and then held at 300 °C for 10 min. The δ^2H values were determined using a ThermoFisher Scientific Delta V IRMS interfaced via a GC Isolink Combustion and High Temperature Conversion interface to a Trace GC Ultra, operating in splitless injection mode (splitless time of 1.5 minutes). Using helium as a carrier gas, 0.5µl of sample was co-injected with 0.5 µl standard (comprising ethyl decanoate and pentadecane), on to a Phenomenx column (ZB-1 30m x 0.25mm x 0.25µm). The temperature program consisted of an initial temperature of 70°C, held for 1 minute, then ramped to 300°C at a rate of 10°Cmin^{-1}, and then held at 300°C for 8 minutes. Isotope measurements are reported using standard delta notation against Vienna Pee Dee Belemnite (VPDB) scale defined by NBS 19 and LSVEC and Vienna Standard Mean Ocean Water (VSMOW) for the ratios $^{13}C/^{12}C$ and D/H,

$$\delta^{13}C = \frac{\left(\frac{^{13}C}{^{12}C}\right)sample}{\left(\frac{^{13}C}{^{12}C}\right)VPDB} - 1\,, \qquad \delta D = \frac{\left(\frac{D}{H}\right)sample}{\left(\frac{D}{H}\right)VPDB} - 1$$

using per mil (‰) units. The precision for $\delta^{13}C$ determinations was ± 0.3 ‰ for natural abundance isotope determinations. The H_3^+ Factor was calculated daily prior to sample analyses and was typically in the range of 1.5-1.8 ppm nA^{-1}. δ^2H values were initially calibrated to two H^2 reference pulses introduced directly into the ion source. All results were subsequently normalised using the equation of linear fit of measured against known δ^2H values of a standard suite of 15 *n*-alkanes (*n*-C_{16} to *n*-C_{30},

https://doi.org/10.5194/egusphere-2024-4021
Preprint. Discussion started: 9 January 2025

Schimmelmann Mixture B3, University of Indiana), which was analysed daily prior to every two sample runs. δ^2H values are reported on the VSMOW-SLAP scale. The instrument residual mean standard error was typically less than 5 ‰, calculated using the same *n*-alkane standard reference. Duplicate analyses of samples were run, with the average of these analyses used as the value for that sample, and the range demonstrated by the bars on Figure 3. In some samples with low concentrations, $\delta^{13}C$ and δ^2H values are based on triplicate measurements.

2. Results

2.1 Distributions of *n*-Alkane plant waxes

In modern environments, *n*-alkanes of specific carbon numbered chain lengths can be used to identify biological sources. Algae and some photosynthetic bacteria produce dominantly *n*-C_{17}, with lesser amounts of *n*-C_{15} and *n*-C_{19} (Clark and Blumer, 1967; Han and Calvin, 1969). Aquatic plants and *Sphagnum* mosses have enhanced production of *n*-C_{23} and *n*-C_{25} (Baas et al., 2000; Pancost et al., 2002). High molecular weight (HMW) *n*-alkanes (*n*-C_{27} and higher), usually with a pronounced odd-over-even predominance (carbon preference index, CPI), mark inputs from the epicuticular leaf and stem waxes of terrestrial higher plants (Eglinton and Hamilton, 1963).

n-Alkane distributions of DSDP 270 sediments are typically bimodal (Fig. 2). We infer compounds in the lower molecular weight range where *n*-C_{17} or *n*-C_{19} are most abundant likely derive from marine algae. High molecular weight *n*-alkanes (*n*-C_{25} to *n*-C_{31}) are characterised by *n*-C_{27} is the most abundant compound. The source and maturity of higher molecular weight *n*-alkanes can be characterised by their carbon preference index (CPI):

$$CPI = \frac{1}{2}\left(\left(\frac{\Sigma_{odd}(n-C_{25-33})}{\Sigma_{even}(n-C_{24-32})}\right) + \left(\frac{\Sigma_{odd}(n-C_{25-33})}{\Sigma_{even}(n-C_{26-34})}\right)\right) \quad (1)$$

A survey of modern leaf wax material demonstrates that a CPI of >1-2 is a reasonable threshold value indicative of relatively unmodified terrestrial plant material (Bush and McInerney, 2013), while sediments containing CPI values of <1 usually indicate either exposure to elevated burial temperatures, or an input of organic matter that has been altered by diagenetic or catagenetic processes (Bray and Evans, 1961). CPI values for *n*-C_{25} to *n*-C_{31} range from 2.4 to 4.4 (avg. = 3.3), indicating they are predominantly sourced from terrestrial plants (Fig. 2).

https://doi.org/10.5194/egusphere-2024-4021
Preprint. Discussion started: 9 January 2025

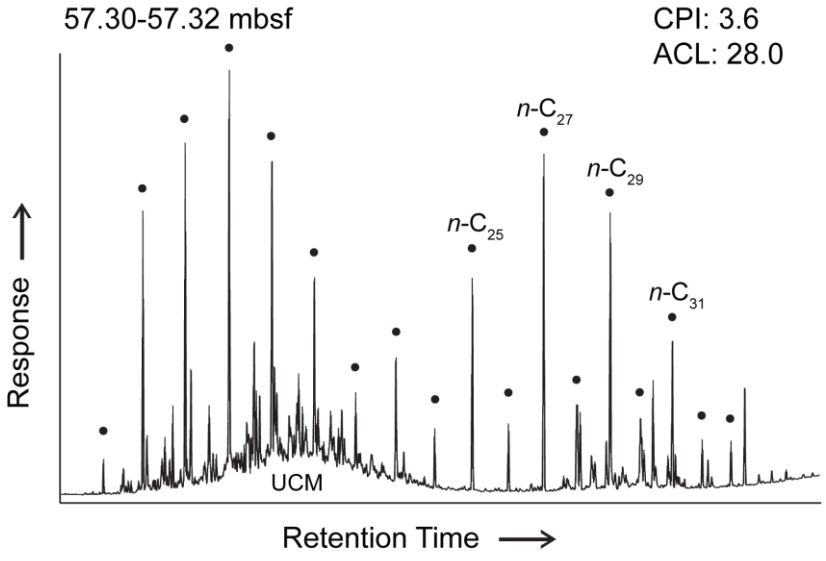

Figure 2: Representative GC-FID chromatogram from DSDP 270. Filled circles above peaks indicate n-alkanes. UCM: Unresolved complex mixture, CPI: Carbon preference index, ACL: Average chain length.

Average chain length (ACL) indicates the dominant *n*-alkane in a given carbon number range (Poynter et al., 1989; Schefuß et al., 2003):

$$ACL = \frac{\Sigma(C_{odd\ 25-33} \cdot x_{odd\ 25-33})}{(x_{odd\ 25-33})} \quad (2)$$

where $C_{odd\ 25\text{-}33}$ represents the carbon number of the odd chain length *n*-alkanes, and $x_{odd\ 25\text{-}33}$ represents the concentrations of the odd *n*-alkanes in the sample. Higher ACLs are typical of warmer, tropical regions, whilst lower ACLs are more commonly observed from cooler, temperate regions, indicating that ACL could be related to air temperature (Gagosian and Peltzer, 1986; Poynter et al., 1989; Dodd and Afzal-Rafii, 2000; Kawamura et al., 2003; Bendle et al., 2007; Vogts et al., 2009; Bush and McInerney, 2015). Other studies suggest that aridity has a strong control on ACL, with the synthesis of longer *n*-alkanes in more arid environments providing plants with a more efficient wax coating to restrict water loss (Schefuß et al., 2003; Dodd et al., 1998; Dodd and Afzal-Rafii, 2000; Calvo et al., 2004; Zhou et al., 2005; Moossen et al., 2015). ACL is also strongly controlled by the contributing vegetation, with large inter- and intra-species variation in *n*-alkane distributions (e.g. Bush and McInerney, 2013; Vogts et al., 2009; Feakins et al., 2016). The ACL values in DSDP 270 vary within a narrow range of ~27.6 to 28, with the lowest values occurring during Mi-1 and in the early Miocene (Fig. 3) (SI Appendix Table S1).

https://doi.org/10.5194/egusphere-2024-4021
Preprint. Discussion started: 9 January 2025

2.2 Plant wax compound specific carbon and hydrogen isotopes

Compound specific carbon isotope ratios were measured for *n*-C_{23} to *n*-C_{31} (SI Appendix Table S2). $\delta^{13}C$ of the odd *n*-alkanes ranges from -25.4 to -38.13 ‰, with most values between -25.8 ‰ and -31.5 ‰. One sample each for *n*-C_{25}, *n*-C_{27} and *n*-C_{29}, and three samples for *n*-C_{31} were excluded as outliers for those specific chain lengths, as they were different from adjacent samples by more than 2 ‰. A marked negative carbon isotope excursion is apparent for all chain lengths across the OMT, with the magnitude of the excursion varying between -2.6 ‰ for *n*-C_{25}, -1.5 ‰ for *n*-C_{27}, -3.5 ‰ for *n*-C_{29} and -5.0 ‰ for *n*-C_{31} (Fig. 3). In more temperate settings *n*-C_{23} and *n*-C_{25} are considered mostly produced by aquatic plants and mosses (Baas et al., 2000, Pancost et al., 2002). However, $\delta^{13}C$ values of *n*-C_{23} and *n*-C_{25} show no correlation (r= 0.13, p=0.5636) at DSDP 270, instead *n*-C_{25} is significantly correlated with the $\delta^{13}C$ of the HMW *n*-alkanes (r=0.84, p=<0.0001 for *n*-C_{25} and *n*-C_{27}, r=0.85, p=<0.0001 for *n*-C_{25} and *n*-C_{29}, and r=0.84, p=<0.0001 for *n*-C_{25} and *n*-C_{31}). This suggests *n*-C_{25} derives from higher plants, as opposed to aquatic plants and mosses. We assume the significant correlation between *n*-C_{25} to *n*-C_{31} to have arisen from a common source, and therefore use an average *n*-alkane value ($\delta^{13}C_{av25\text{-}31}$) to discuss the trend. The magnitude of the negative excursion between $\delta^{13}C_{av25\text{-}31}$ values in the upper Oligocene and Mi-1 is -2.9 ‰ (Fig. 3).

Hydrogen compound specific isotopes were measured on *n*-C_{23} to *n*-C_{31} *n*-alkanes (SI Appendix Table S2). The $\delta^{2}H$ values of the odd chain lengths vary from -144 to -207 ‰. Similar to $\delta^{13}C$, *n*-C_{23} and *n*-C_{25} show no correlation (r=0.12, p=0.6507), instead *n*-C_{25} is significantly correlated with the $\delta^{2}H$ of the HMW *n*-alkanes, albeit to a weaker extent than $\delta^{13}C$ (r=0.67, p=0.0001 for *n*-C_{25} and *n*-C_{27}, r=0.53, p=0.0046 for *n*-C_{25} and *n*-C_{29}, and r=0.42, p=0.0312 for *n*-C_{25} and *n*-C_{31}). Like $\delta^{13}C$, we interpret *n*-C_{25} to *n*-C_{31} as sourced from terrestrial vegetation and take an average $\delta^{2}H$ value across these chain lengths to investigate $\delta^{2}H$ trends. We find a shift to more positive values between upper Oligocene sediments and Mi-1, with the exception of more negative values in samples at 174 mbsf and 133 mbsf (Fig. 3).

https://doi.org/10.5194/egusphere-2024-4021
Preprint. Discussion started: 9 January 2025

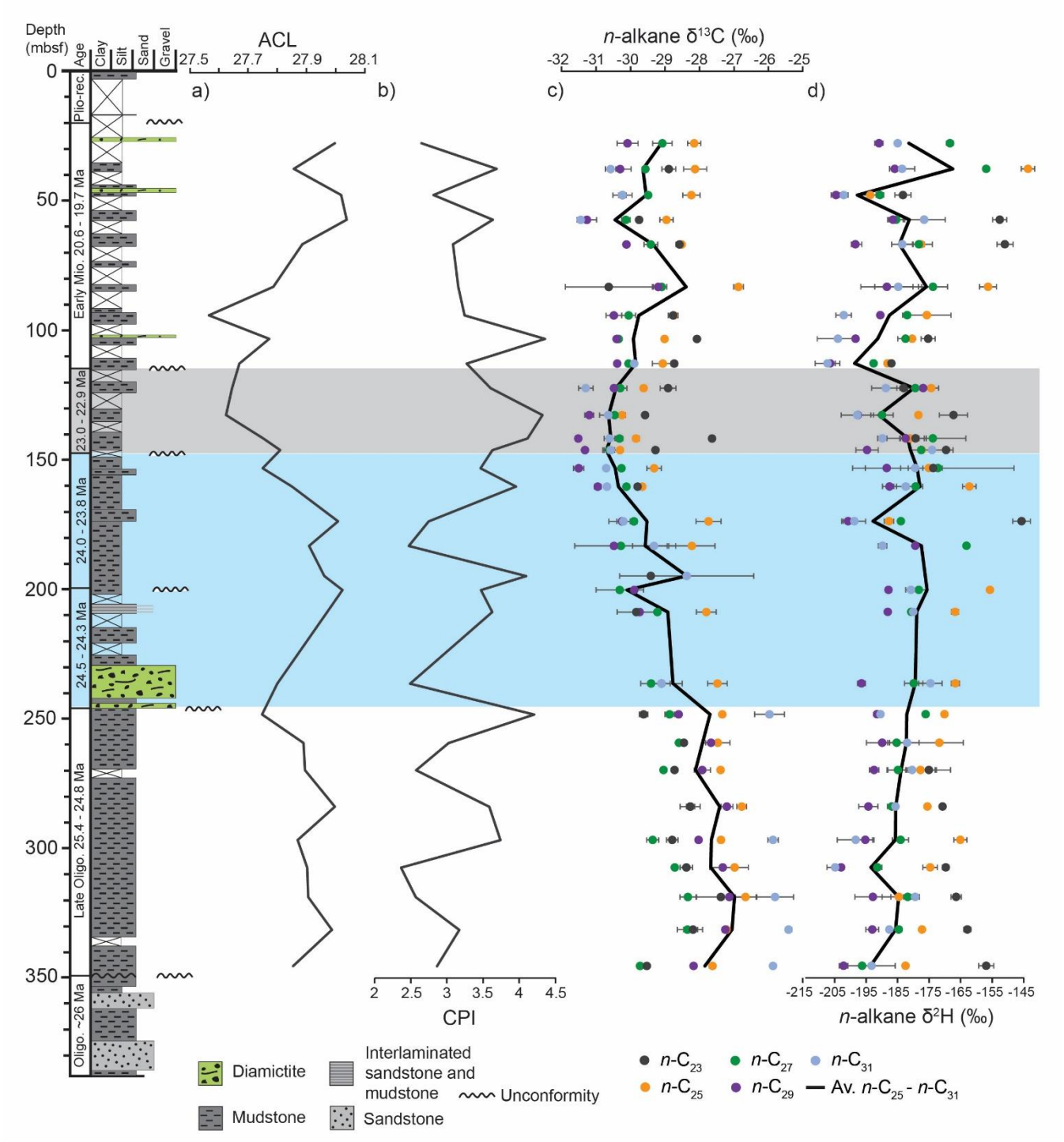

Figure 3: Stratigraphy of DSDP 270 with a) average chain length values for n-alkanes, b) carbon preference index for n-alkanes c) n-alkane $\delta^{13}C$, d) n-alkane $\delta^{2}H$. Error bars on c) and d) represent the range of analyses for that sample. Black lines on c) and d)

https://doi.org/10.5194/egusphere-2024-4021
Preprint. Discussion started: 9 January 2025

show the average value for *n*-C_{25} to *n*-C_{31}. The blue box represents an interval of regional cooling, while the grey box indicates the interval containing Mi-1.

3. Discussion

3.1 Antarctic vegetation during the OMT.

Palynological analysis indicates a low diversity, shrubby tundra dominated by *Nothofagidites*, podocarps and bryophytes (including mosses) persisting during sediment deposition at DSDP 270 (Kulhanek et al., 2019). Pollen assemblages are sparse with low pollen counts, but available data indicate only minor changes in vegetation diversity during Mi-1, with a relative increase of spores sourced from mosses and other bryophytes (Kulhanek et al., 2019) (Fig. 4). Palynological assemblages contain minimal reworked taxa, which is supported by *n*-alkane CPI values above 2.4 indicating plant waxes reflect contemporaneous Oligocene/Miocene input rather than a reworked source (SI Appendix Text, Duncan et al., 2019; Kulhanek et al., 2019). The ACL values between 27.6 and 28 are also consistent with other Oligocene and Miocene-aged Antarctic sediments that typically contain *n*-C_{27} as the dominant HMW *n*-alkane (Duncan et al., 2019). The lowest ACL values occur in Mi-1 and the early Miocene and are likely driven by climate (i.e. cooler temperatures) with some impact due to the minor vegetation change that pollen assemblages suggest occurred during this interval.

3.2 Drivers of carbon isotope discrimination in Antarctic plants

The carbon isotopic composition of plant leaf waxes is the product of the atmospheric CO_2 carbon source ($\delta^{13}C_{atm}$) and kinetic isotope effects associated with photosynthesis, carbon fixation and other plant biochemical processes, that result in more negative $\delta^{13}C$ in plant matter relative to atmospheric CO_2 (Farquhar et al., 1989; Marshall et al., 2007). Modern plants typically employ either the C_3, C_4 or CAM photosynthetic pathway to assimilate carbon, with each pathway resulting in different bulk plant carbon isotopic compositions (Marshall et al., 2007). C_4 plants did not become a significant component of Earth's biosphere until the late Miocene, and modern high latitudes still overwhelming comprise C_3 vegetation, with C_4 and CAM plants inhabiting warm, arid lower latitude environments (Tipple and Pagani, 2007; Polissar et al., 2019). As such, only C_3 plants likely comprised the Antarctica vegetation of the late Oligocene and early Miocene.

In the leaves of C_3 plants, carbon discrimination (Δ) is described by the relationship:

$$\Delta = a + (b - a) \times p_i/p_a \quad (3)$$

https://doi.org/10.5194/egusphere-2024-4021
Preprint. Discussion started: 9 January 2025

Where a is a fractionation of 4.4 ‰ caused by the diffusion of CO_2 from the atmosphere into the stomata, b is the photosynthetic fractionation by Rubisco of 27 ‰, and p_i/p_a is the ratio between the partial pressure of CO_2 in the leaf (p_i) to the atmosphere (p_a) (Farquhar et al., 1989).

The magnitude of carbon isotope discrimination (Δ) across the O/M transition can be described by the difference between the $\delta^{13}C_{atm}$, and the $\delta^{13}C$ incorporated into the plant ($\delta^{13}C_{TT}$) (Farquhar et al., 1989):

$$\Delta = \frac{\delta^{13}C_{atm} - \delta^{13}C_{TT}}{1 + \frac{\delta^{13}C_{TT}}{1000}} \quad (4)$$

For $\delta^{13}C_{atm}$ we use the 0.5 Myr moving average derived from for benthic foraminifera from Tipple et al. (2010). We use benthic foraminiferal values as they are not affected by differences in production depth, the impact of photosymbiotes or seasonal variability (Tipple et al., 2010). A potential source of error in using this method is that the same $\delta^{18}O_{sw}$ value (-0.5 ‰) is applied over the late Oligocene and early Miocene during the calculation of $\delta^{13}C_{atm}$. It is likely this value would have varied in response to ice volume changes, but Tipple et al. (2010) consider the impact of this on the calculated $\delta^{13}C_{atm}$ to be minor. To calculate the carbon isotopic value of the total plant tissue ($\delta^{13}C_{TT}$), an enrichment factor is applied to account for isotopic fractionation between plant tissue and individual *n*-alkanes (ε_{lipid}). This is calculated by applying *n*-alkane specific averages from published data for temperate C_3 plants (Collister et al., 1994; Chikaraishi and Naraoka, 2003; Diefendorf et al., 2011). The ε_{lipid} corrections applied are 3.28 ‰ for *n*-C_{25}, 3.46 ‰ for *n*-C_{27}, 3.90 ‰ for *n*-C_{29} and 4.17 ‰ for *n*-C_{31}, with the average of these values (3.70 ‰) applied to the $\delta^{13}C_{av25\text{-}31}$ record. This method determines a positive shift in Δ over the OMT (Fig. 4). The magnitude of this change varies between 3.06 ‰ for *n*-C_{25}, 1.93 ‰ for *n*-C_{27}, 3.94 ‰ for *n*-C_{29} and 5.54 ‰ for *n*-C_{31}, with a value of 3.38 ‰ for $\delta^{13}C_{av25\text{-}31}$.

In modern global datasets, Δ is largely linked to water availability. Water stress causes plants to reduce stomatal width to combat evapotranspiration, thereby limiting the diffusion of CO_2 into the leaf, and resulting in smaller carbon isotope discrimination (Marshall et al., 2007). Changes in Δ are therefore usually associated with an array of environmental factors that cumulatively influence the supply and demand for water, for example, precipitation, potential evapotranspiration, temperature, elevation and plant species-specific traits (e.g. Diefendorf et al., 2010; Kohn 2010; Cornwell et al., 2018; Basu et al. 2019).

https://doi.org/10.5194/egusphere-2024-4021
Preprint. Discussion started: 9 January 2025

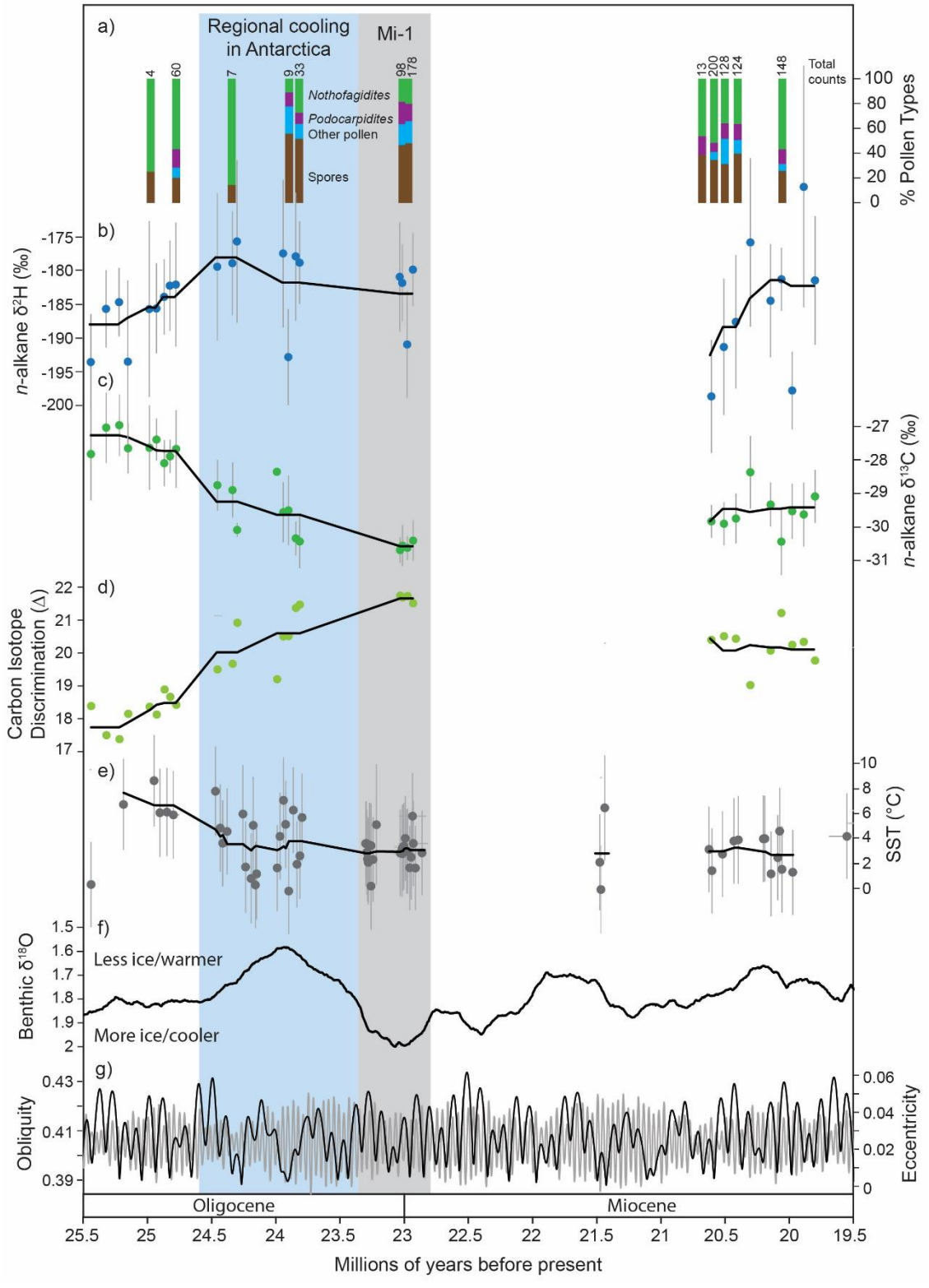

https://doi.org/10.5194/egusphere-2024-4021
Preprint. Discussion started: 9 January 2025

Figure 4: a) Percentages of pollen groupings from 16, numbers represent total counts of pollen in each sample, b) n-Alkane δ^2H average from *n*-C_{25} to *n*-C_{31}, 1σ error bars represent the variance in different chain lengths used to reconstruct the average values, c) n-Alkane $\delta^{13}C$ average from *n*-C_{25} to *n*-C_{31}, 1σ error bars represent the variance in different chain lengths used to reconstruct the average values, d) Carbon isotope discrimination, e) Compilation of sea surface temperatures from the Ross Sea (GDGT-based OPTiMAL calibration) (Duncan et al., 2022) f) 500 kyr moving average of benthic δ18O from Westerhold et al. (2020) g) Obliquity in radians, in light grey from Laskar et al. (2004), and eccentricity in black from (Laskar et al. 2011). Black moving averages for a)-f) are 500 kyr moving averages derived using mwStats in the R package astrochron (Meyers et al. (2019).

We take a modern analogue approach to consider the environmental and species-specific factors that would have impacted Δ in Antarctic vegetation during the OMT. Our fossil pollen assemblage is dominated by *Nothofagidites* species, with *Podocarpidites* also a persistent feature through the drill core (Kulhanek et al., 2019). Differences in Δ are apparent across various modern species and plant functional types, with $\delta^{13}C_{alkanes}$ from angiosperms typically ~3-5 ‰ more depleted than gymnosperms (Chikaraishi and Naraoka, 2003; Diefendorf et al., 2011). However, pollen from DSDP 270 and other Ross Sea sections do not indicate a significant change in the proportion of angiosperms (i.e. *Nothofagidites*) and gymnosperms (i.e. *Podocarpidites*) across the OMT (Askin and Raine, 2000; Prebble et al., 2006; Kulhanek et al., 2019), leading us to discount a change in vegetation assemblage as a key driver of our Δ trend.

In modern environments, Δ in Nothofagaceae and Podocarpaceae has a variable response to precipitation. For example, high latitude Nothofagaceae have been shown to have higher Δ during summer despite lower rainfall, suggesting physiological or morphological adaption to allow continued photosynthesis during the warm conditions of summer despite mild water deficit (Read and Farquhar, 1991; Read et al., 2010). In contrast, other studies using *in situ* and herbarium Nothofagaceae, as well as Podocarpaceae, have described decreased plant $\delta^{13}C$ and thus increased Δ in response to increased precipitation (Peri et al., 2012; Griener et al., 2013; Brett et al., 2014). However, modern Nothofagaceae and Podocarpaceae are likely imperfect analogues for vegetation in DSDP 270, as these plants exist at lower latitudes under different light and growing season conditions than would have been experienced by Antarctic vegetation during the OMT.

This leads us to consider modern Arctic vegetation as an analogue for ancient Antarctic vegetation. Like the modern Arctic, at latitudes south of the Antarctic Circle, growth would be restricted to a short period during summer when there was sunlight, thawed soil and warmer temperatures for photosynthesis. Low precipitation is not necessarily restrictive in modern high Arctic environments, as key water sources are snow melt and permafrost thawing at the base of the active soil layer (Gold and Bliss, 1995). Therefore, growth is heavily influenced by soil and air temperature as well as nutrient levels (e.g. Gold and Bliss, 1995; Sturm et al., 2005; Ernakovich et al., 2014). For example, higher Δ correlates with colder temperatures in *Carex* from the Eurasian coastal Arctic (Welker et al., 2003). We suggest a restricted Antarctic summer growing season required plants to retain open stomata to allow continued uptake of CO_2, thereby prioritising the assimilation of CO_2 over water use efficiency, leading to elevated carbon isotope discrimination. The summer growing window would be further constrained in the latest

https://doi.org/10.5194/egusphere-2024-4021
Preprint. Discussion started: 9 January 2025

Oligocene by colder temperatures associated with reduced atmospheric pCO_2 concentrations (CenCO2PIP, 2023) coupled with orbital conditions (i.e. reduced eccentricity and obliquity) favouring low seasonality (Fig. 5.). Additionally, low intensity, high latitude continuous light conditions result in more negative plant $\delta^{13}C$ values than for plants living under diurnal light (Yang et al., 2009). Taken together, low seasonality and decreased light intensity during the OMT would contribute to a negative $\delta^{13}C$ excursion and associated higher Δ (Fig. 5).

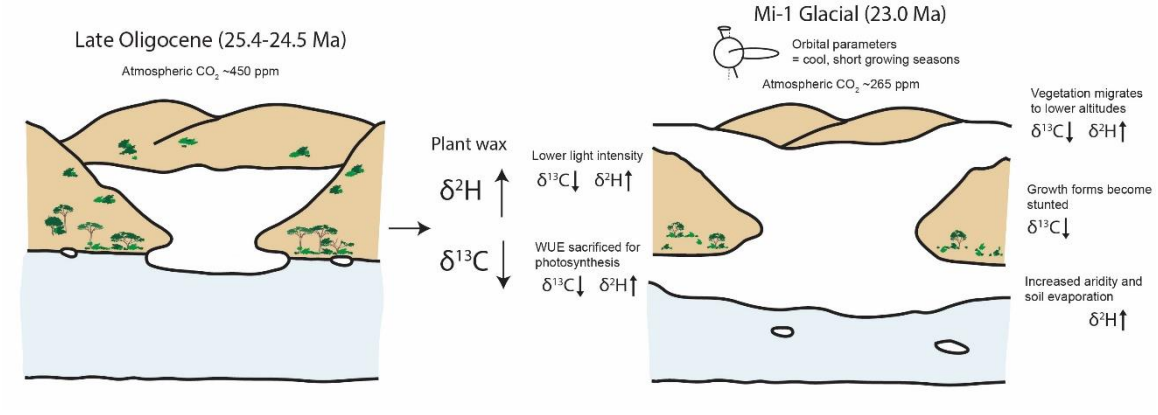

Figure 5: Summary of interpreted drivers for isotopic trends in DSDP 270. WUE= water use efficiency.

Other environmental conditions of relevance to the OMT in Antarctica could also increase Δ. Plants living at lower elevations typically display higher Δ, influenced by variation in the partial pressure of CO_2 and O_2, humidity, temperature, irradiance or other factors (e.g. Diefendorf et al., 2010; Wu et al., 2017). During large transient glaciations like Mi-1 it is likely vegetation became restricted to low elevation coastal regions due to ice advance and climatic controls, resulting in the DSDP 270 terrestrial catchment area integrating an increase in average Δ. Tree height can also impact Δ, with declining values a function of increasing tree height in a global dataset (McDowell et al., 2011). For example, Δ varies with Nothofagaceae tree height on the order of -0.22 ‰/m in New Zealand (McDowell et al., 2011). During a cold glacial period in Antarctica, tree species like *Nothofagidites* would adapt by stunting their growth, forming shrub-like forms similar to Antarctic Miocene or Pliocene-aged *Nothofagidites* fossils preserved at Oliver Bluffs in the Beardmore Glacier region (Francis and Hill, 1996).

The response of Δ to changes in atmospheric pCO_2 has been extensively debated, with variable results from recent observations, laboratory experiments, and Cenozoic fossil evidence (e.g. Arens et al., 2000; Schubert and Jahren, 2015; Lomax et al., 2019; Schlanser et al., 2020). A Last Glacial Maximum to Holocene global compilation of Schubert and Jahren (2015) suggests a positive relationship between Δ and pCO_2. Their global compilation record averages the effects of local and regional environmental conditions and plant community shifts, and results in a trend best explained by changing pCO_2. However, as DSDP 270 reflects a highly specific regional signal it is not interpreted in these terms. Furthermore, a positive relationship

https://doi.org/10.5194/egusphere-2024-4021
Preprint. Discussion started: 9 January 2025

between Δ in DSDP 270 and pCO_2 would be in opposition to independent proxy records that exhibit declining pCO_2 through the late Oligocene (CenCO2PIP, 2023).

3.3 Hydrogen isotopes in Antarctica plants as an indicator of hydroclimate

Leaf wax lipid hydrogen isotope signatures (δ^2H_l) are highly correlated with, but significantly offset from their plant's water source, typically meteoric water (δ^2H_w) (Sessions et al., 1999; Sachse et al., 2004). The δ^2H_w varies spatially and temporally due to Rayleigh fractionation processes resulting from rainfall, temperature, orographic effects and distance from water source (Sachse et al. 2012). In modern ecosystems, wetter conditions are associated with more negative δ^2H_w in the low latitudes, but at mid- to high-latitudes δ^2H_w is more strongly linked to temperature gradients, with more positive δ^2H_w recorded at warmer temperatures (Bowen, 2008; Masson-Delmotte et al., 2008). Soil water is the main water source for terrestrial higher plants and predominantly reflects an amount weighted average of precipitation inputs. However, the uppermost soil horizons can have ^2H enrichment due to evaporation (Sachse et al., 2012). While there is typically no fractionation between source water and root uptake, leaf composition can have a wide range of variability due to transpiration, and fractionation that further occurs during biosynthesis of leaf wax lipids (Sessions et al., 1999; Chikaraishi and Naraoka, 2003; Kahmen et al., 2013a; 2013b). The hydrogen isotopic composition of lipids can show a large variation when measured on individual organisms, but analysing sediment results in significantly reduced variability due to spatial and temporal integration in the catchment (Sachse et al., 2012).

In DSDP 270, plant wax δ^2H values trend from more negative in the late Oligocene to more positive over the OMT (Figs. 3 and 4). This suggests temperature is unlikely to be the dominant control on plant wax δ^2H at this site, as more positive values would indicate warmer temperatures in the middle of a large glacial interval, contradicting sea surface temperature records for the Ross Sea and a range of other paleoenviromental and sedimentological evidence for cool conditions during this time (Leckie and Webb, 1983; Naish et al., 2001; Duncan et al., 2022). Instead, we suggest the observed ^2H enrichment results from shorter, colder and more arid growing seasons. Evidence for this comes from studies of ^2H incorporation into high latitude plants and plant waxes, which, similar to $\delta^{13}C$, demonstrate that plants living under low intensity, continuous light conditions at high latitudes show smaller fractionations of hydrogen between leaf waxes and their water source than mid- to low-latitude plants due to high transpiration rates as plants continuously photosynthesise during 24 hr light conditions (Yang et al., 2009; 2011; Shanahan et al., 2013). A shift to more positive δ^2H_l values during the late Eocene on the Antarctic Peninsula (Feakins et al., 2014) and the Eocene/Oligocene transition from Prydz bay (Tibbett et al., 2021) are also interpreted as reflecting smaller fractionations in response to cooling, drying and a shift towards more tundra-like vegetation. We therefore conclude that low seasonality, decreased light intensity and more arid conditions during the OMT resulted in even smaller hydrogen isotope fractionation and consequently more positive δ^2H_l, as enhanced plant transpiration occurred at the expense of water use efficiency to allow plants to photosynthesise during shorter, harsh growing seasons (Fig. 5.).

https://doi.org/10.5194/egusphere-2024-4021
Preprint. Discussion started: 9 January 2025

Other environmental factors likely also impacted positive δ^2H values. Studies on Miocene or Pliocene macrofossils from Oliver Bluffs in the Transantarctic Mountains indicate that shallow-rooted, stunted tundra vegetation grew on permafrost with restricted drainage in arid conditions (Francis and Hill, 1996; Ashworth and Cantrill, 2004). Using this as an analogue for the Ross Sea region during the OMT we infer plants would have incorporated higher proportions of ^2H as arid conditions and poor drainage led to ^2H enrichment in the uppermost soil layers. Plants were also likely restricted to lower elevations as a consequence of the colder climate and increased ice volume during Mi-1, a process which also drives δ^2H_l towards more positive values (Fig. 5. Polissar et al., 2009)).

4. Synthesis

We present a proximal Antarctic record of the OMT including the Mi-1 glaciation, one of the largest transient glacial excursions of the Cenozoic. We find a marked negative $\delta^{13}C$ excursion in HMW *n*-alkanes, coincident with a shift to more positive *n*-alkane δ^2H. These trends begin ~24.5 Ma, coinciding with cooling Ross Sea temperatures and the deposition of glacially proximal sediments in DSDP 270 (Fig. 4, Kulhanek et al., 2019; Duncan et al., 2022; Olivetti et al., 2023). This is inferred to represent the first significant marine ice sheet advance of the late Oligocene, occurring in response to atmospheric CO_2 declining below 450-400 ppm and an astronomical configuration optimal for ice sheet growth (Duncan et al., 2022; Olivetti et al., 2023).

The most negative *n*-alkane $\delta^{13}C$ and most positive δ^2H in DSDP 270 occurred during the latest Oligocene and the Mi-1 event, when the AIS increased to an even greater size during another period with a favourable astronomical configuration and a further decline in CO_2 to ~265 ppm (Greenop et al., 2019, CenCO2PIP, 2023). We attribute *n*-alkane $\delta^{13}C$ and δ^2H trends to several environmental changes that affected Antarctic vegetation during the OMT (Fig. 5.). These are: 1) a shift in climate to colder, shorter and more arid growing seasons with lower light intensity, 2) a decrease in catchment area and reduction in growing region (both space and elevation), 3) a shift to more shrub-like growth forms. The impact of growing season length and conditions on the isotopic trends demonstrated during the OMT likely indicates Antarctic plants prioritised continued photosynthesis and uptake of carbon over water use efficiency during the short growing season. Plant wax isotopic records from DSDP 270 provide insight into the response and survival mechanisms of Antarctic vegetation during major glacial expansion. Importantly, data from this past interval of warmer-than-present climate suggest that a range of vascular plants and shrubs are capable of establishing a foothold in Antarctic under atmospheric CO_2 levels comparable to present. Although vegetation continued to subsist on the continent following Mi-1, this glacial period marked a key step towards the eventual demise of nearly all vegetation in Antarctica as increasingly polar conditions developed over the course of the Cenozoic.

https://doi.org/10.5194/egusphere-2024-4021
Preprint. Discussion started: 9 January 2025

Data availability

Data will be archived in a data repository (Pangaea) upon publication of the preprint. All data is also available in the supplementary files for review.

Author contributions

B.D., R.M., J.B., R.L. and T.N. designed the research. B.D. processed samples and conducted analysis for DSDP 270. J.G.P. assisted with vegetation and environmental interpretations. O.S. and G.T.V. assisted with plant wax distribution and isotope interpretations. H.M. advised on laboratory processing and data interpretation. C.K. and D.K.K. assisted with sedimentological and environmental interpretations. B.D. wrote the text and created the figures with assistance from all authors.

Competing interests

The authors declare that they have no conflict of interest.

Acknowledgments

The authors are grateful for access to samples from the IODP core repository at Texas A&M University and GNS Science for DSDP Site 270. This study was funded via an Antarctica New Zealand Sir Robin Irvine PhD Scholarship, Scientific Committee of Antarctic Research Fellowship and Rutherford Foundation Postdoctoral Fellowship (RFT-VUW1804-PD) awarded to B.D, with additional funding by the Royal Society Te Apārangi Marsden Fund award MFP-VUW1808 and New Zealand Ministry of Business, Innovation and Employment through the Antarctic Science Platform (ANTA1801) (B.D., R.M., T.N., R.L., J.G.P.). Isotope analysis was performed at the NERC- Life Sciences Mass Spectrometry Facility at the University of Bristol (project BRIS/85/1015), we thank Hanna Gruszczynska for laboratory support. The authors are grateful for support from IODP and support in kind from the University of Birmingham.

References

Arens, N. C., Jahren, A. H., and Amundson, R.: Can C_3 plants faithfully record the carbon isotopic composition of atmospheric carbon dioxide?, Paleobiology, 26, 137-164, 2000.

Ashworth, A. C. and Cantrill, D. J.: Neogene vegetation of the Meyer Desert Formation (Sirius Group) Transantarctic Mountains, Antarctica, Palaeogeogr. Palaeoclimatol. Palaeoecol., 213, 65-82, 2004.

https://doi.org/10.5194/egusphere-2024-4021
Preprint. Discussion started: 9 January 2025

Baas, M., Pancost, R., van Geel, B., and Sinninghe Damsté, J.S.: A comparative study of lipids in Sphagnum species, Org. Geochem., 31, 535-541, 2000.

Barrett, P. J.: Resolving views on Antarctic Neogene glacial history–the Sirius debate, Earth Environ. Sci. Trans. R. Soc. Edinb., 104, 31-53, 2013

Basu, S., Ghosh, S., and Sanyal, P.: Spatial heterogeneity in the relationship between precipitation and carbon isotopic discrimination in C3 plants: Inferences from a global compilation, Global Planet. Change, 176, 123-131, 2019.

Beddow, H. M., Liebrand, D., Sluijs, A., Wade, B. S., and Lourens, L. J.: Global change across the Oligocene-Miocene transition: High-resolution stable isotope records from IODP Site U1334 (equatorial Pacific Ocean), Paleoceanography, 31, 81-97, 2016.

Bendle, J., Kawamura, K., Yamazaki, K., and Niwai, T.: Latitudinal distribution of terrestrial lipid biomarkers and n-alkane compound-specific stable carbon isotope ratios in the atmosphere over the western Pacific and Southern Ocean. Geochim. Cosmochim. Acta, 71, 5934-5955, 2007.

Bowen, G. J.: Spatial analysis of the intra-annual variation of precipitation isotope ratios and its climatological corollaries, J. Geohys. Res., Atmos., 113, D05113, doi:10.1029/2007JD009295, 2008.

Bray, E.E., and Evans, E.D.: Distribution of n-paraffins as a clue to recognition of source beds, Geochim. Cosmochim. Acta, 22, 2-15, 1961.

Brett, M. J., Baldini, J. U., and Gröcke, D. R.: Environmental controls on stable isotope ratios in New Zealand Podocarpaceae: Implications for palaeoclimate reconstruction, Global Planet. Change, 120, 38-45, 2014.

Bush, R. T., and McInerney, F. A.: Leaf wax n-alkane distributions in and across modern plants: implications for paleoecology and chemotaxonomy, Geochim. Cosmochim. Acta, 117, 161-179, 2013.

Bush, R. T., and McInerney, F. A.: Influence of temperature and C_4 abundance on n-alkane chain length distributions across the central USA, Org. Geochem., 79, 65-73, 2015.

Calvo, E., Pelejero, C., Logan, G. A., and De Deckker, P.: Dust-induced changes in phytoplankton composition in the Tasman Sea during the last four glacial cycles, Paleoceanography

, 19, PA2020, doi:10.1029/2003PA000992, 2004.

Cenozoic CO2 Proxy Integration Project (CenCO2PIP) Consortium: Toward a Cenozoic history of atmospheric CO_2, Science, 382, eadi5177, 2003.

Clark Jr, R. C., and Blumer, M.: Distribution of n-paraffins in marine organisms and sediment, Limnol. Oceanogr., 12, 79-87, 1967.

https://doi.org/10.5194/egusphere-2024-4021
Preprint. Discussion started: 9 January 2025

Chikaraishi, Y., and Naraoka, H.: Compound-specific δD–δ^{13}C analyses of n-alkanes extracted from terrestrial and aquatic plants, Phytochem., 63, 361-371, 2003.

Colesie, C., Walshaw, C. V., Sancho, L. G., Davey, M. P., and Gray, A.: Antarctica's vegetation in a changing climate, WIREs Clim. Change, 14, e810, 2023.

Collister, J. W., Rieley, G., Stern, B., Eglinton, G., and Fry, B.: Compound-specific δ^{13}C analyses of leaf lipids from plants with differing carbon dioxide metabolisms, Org. Geochem., 21, 619-627, 1994.

Cornwell, W. K., Wright, I. J., Turner, J., Maire, V., Barbour, M. M., Cernusak, L. A., Dawson, T., Ellsworth, D., Farquhar, G. D., Griffiths, H., Keitel, C., Knohl, A., Reich, P. B., Williams, D. G., Bhaskar, R., Cornelissen, J. H. C., Richards, A., Schmidt, S., Valladares, F., Körner, C., Schulze, E.-D., Buchmann, N. and Santiago, L. S.: Climate and soils together regulate photosynthetic carbon isotope discrimination within C_3 plants worldwide, Glob. Ecol. Biogeogr., 27, 1056-1067, 2018.

De Santis, L., Prato, S., Brancolini, G., Lovo, M., and Torelli, L.: The Eastern Ross Sea continental shelf during the Cenozoic: implications for the West Antarctic ice sheet development, Global Planet. Change, 23, 173-196, 1999.

Diefendorf, A. F., Mueller, K. E., Wing, S. L., Koch, P. L., and Freeman, K. H.: Global patterns in leaf ^{13}C discrimination and implications for studies of past and future climate, PNAS, 107, 5738-5743, 2010.

Diefendorf, A. F., Freeman, K. H., Wing, S. L., and Graham, H. V.: Production of n-alkyl lipids in living plants and implications for the geologic past, Geochim. Cosmochim. Acta, 75, 7472-7485, 2011.

Dodd, R. S., Rafii, Z. A., and Power, A. B.: Ecotypic adaptation in Austrocedrus chilensis in cuticular hydrocarbon composition, New Phytol., 138, 699-708, 1998.

Dodd, R. S., and Afzal-Rafii, Z.: Habitat-related adaptive properties of plant cuticular lipids, Evolution, 54, 1438-1444, 2000.

Duncan, B., McKay, R., Bendle, J., Naish, T., Inglis, G. N., Moossen, H., Levy, R., Ventura, G. T., Lewis, A., Chamberlain. B. and Walker, C.: Lipid biomarker distributions in Oligocene and Miocene sediments from the Ross Sea region, Antarctica: Implications for use of biomarker proxies in glacially-influenced settings, Palaeogeogr. Palaeoclimatol. Palaeoecol., 516, 71-89, 2019.

Duncan, B., McKay, R., Levy, R., Naish, T., Prebble, J. G., Sangiorgi, F., Krishnan, S., Hoem, F., Clowes, C., Dunkley Jones, T., Gasson, E., Kraus, C., Kulhanek, D. K., Meyers, S. R., Moossen, H., Warren, C., Willmott, V., Ventura, G. T., and Bendle, J.: Climatic and tectonic drivers of late Oligocene Antarctic ice volume, Nat. Geosci., 15, 819-825, 2022.

Eglinton, G., and Hamilton, R. J.: The distribution of alkanes, Chem. plant taxon., 187, 217, 1963.

https://doi.org/10.5194/egusphere-2024-4021
Preprint. Discussion started: 9 January 2025

Ernakovich, J. G., Hopping, K. A., Berdanier, A. B., Simpson, R. T., Kachergis, E. J., Steltzer, H., and Wallenstein, M. D.: Predicted responses of arctic and alpine ecosystems to altered seasonality under climate change, Glob. Change Biol., 20, 3256-3269, 2014.

Farquhar, G. D., Ehleringer, J. R., and Hubick, K. T.: Carbon isotope discrimination and photosynthesis, Annu. Rev. Plant Biol., 40, 503-537, 1989.

Feakins, S. J., Warny, S., and DeConto, R. M.: Snapshot of cooling and drying before onset of Antarctic Glaciation, Earth Planet. Sci. Lett., 404, 154-166, 2014.

Feakins, S. J., Peters, T., Wu, M. S., Shenkin, A., Salinas, N., Girardin, C. A., Bentley, L. P., Blonder, B., Enquist, B. J., Martin, R. E., Asner, G. P., and Asner, G. P.: Production of leaf wax n-alkanes across a tropical forest elevation transect, Org. Geochem., 100, 89-100, 2016.

Fielding, C. R., Harwood, D. M., Winter, D. M., and Francis, J. E.: Neogene stratigraphy of Taylor Valley, Transantarctic Mountains, Antarctica: evidence for climate dynamism and a vegetated early Pliocene coastline of McMurdo Sound, Global Planet. Change, 96, 97-104, 2012.

Francis, J.E., and Hill, R.S.: Fossil plants from the Pliocene Sirius Group, Transantarctic Mountains: Evidence for climate from growth rings and fossil leaves, Palaios, 11, 389-396, 1996.

Gagosian, R. B., and Peltzer, E. T.: The importance of atmospheric input of terrestrial organic material to deep sea sediments, Org. Geochem., 10, 661-669, 1986.

Gold, W. G., and Bliss, L. C.: Water limitations and plant community development in a polar desert, Ecology, 76, 1558-1568, 1995.

Greenop, R., Sosdian, S. M., Henehan, M. J., Wilson, P. A., Lear, C. H., and Foster, G. L.: Orbital forcing, ice volume, and CO_2 across the Oligocene-Miocene transition, Paleoceanogr. Paleoclimatol., 34, 316-328, 2019.

Griener, K. W., Nelson, D. M., and Warny, S.: Declining moisture availability on the Antarctic Peninsula during the Late Eocene, Palaeogeogr. Palaeoclimatol. Palaeoecol., 383, 72-78, 2013.

Han, J., and Calvin, M.: Hydrocarbon distribution of algae and bacteria, and microbiological activity in sediments. PNAS, 64, 436-443, 1969.

Kahmen, A., Schefuß, E., and Sachse, D.: Leaf water deuterium enrichment shapes leaf wax n-alkane δD values of angiosperm plants I: Experimental evidence and mechanistic insights, Geochim. Cosmochim. Acta, 111, 39-49, 2013a.

Kahmen, A., Hoffmann, B., Schefuß, E., Arndt, S. K., Cernusak, L. A., West, J. B., and Sachse, D.: Leaf water deuterium enrichment shapes leaf wax n-alkane δD values of angiosperm plants II: Observational evidence and global implications, Geochim. Cosmochim. Acta, 111, 50-63, 2013b.

https://doi.org/10.5194/egusphere-2024-4021
Preprint. Discussion started: 9 January 2025

Kawamura, K., Ishimura, Y., and Yamazaki, K.: Four years' observations of terrestrial lipid class compounds in marine aerosols from the western North Pacific, Global Biogeochem. Cycles, 17, 2003.

Kohn, M. J.: Carbon isotope compositions of terrestrial C_3 plants as indicators of (paleo) ecology and (paleo) climate, PNAS, 107, 19691-19695, 2010.

Kulhanek, D. K., Levy, R. H., Clowes, C. D., Prebble, J. G., Rodelli, D., Jovane, L., Morgans, H. E. G., Kraus, C., Zwingmann, H., Griffith, E. M., Scher, H. D., McKay, R. M., and Naish, T. R.: Revised chronostratigraphy of DSDP Site 270 and late Oligocene to early Miocene paleoecology of the Ross Sea sector of Antarctica, Global Planet. Change, 178, 46-64, 2019.

Laskar, J., Robutel, P., Joutel, F., Gastineau, M., Correia, A. C. M., and Levrard, B.: A long-term numerical solution for the insolation quantities of the Earth, A&A, 428, 261-285, 2004.

Laskar, J., Fienga, A., Gastineau, M., and Manche, H.: La2010: a new orbital solution for the long-term motion of the Earth, A&A, 532, A89, 2011.

Leckie, R. M., and Webb, P. N.: Late Oligocene–early Miocene glacial record of the Ross Sea, Antarctica: Evidence from DSDP site 270, Geology, 11, 578-582, 1983.

Lewis, A. R., Marchant, D. R., Ashworth, A. C., Hedenäs, L., Hemming, S. R., Johnson, J. V., Leng, M. J., Machlus, M. L., Newton, A. E., Raine, J. I., Willenbring, J. K., Williams, M., and Wolfe, A. P.: Mid-Miocene cooling and the extinction of tundra in continental Antarctica, PNAS, 105, 10676-10680, 2008.

Lomax, B. H., Lake, J. A., Leng, M. J., and Jardine, P. E.: An experimental evaluation of the use of $\Delta^{13}C$ as a proxy for palaeoatmospheric CO_2, Geochim. Cosmochim. Acta, 247, 162-174, 2019.

Marshall, J. D., Brooks, J. R., and Lajtha, K.: Sources of variation in the stable isotopic composition of plants. In R. Michener and K Lajtha (Eds), Stable isotopes in ecology and environmental science (pp. 22-60). Oxford: Blackwell Publishing, 2007.

Masson-Delmotte, V., Hou, S., Ekaykin, A., Jouzel, J., Aristarain, A., Bernardo, R. T., Bromwich, D., Cattani, O., Delmotte, M., Falourd, S., Frezzotti, M., Gallée, H., Genoni, L., Isaksson, E., Landais, A., Helsen, M. M., Hoffmann, G., Lopez, J., Morgan, V., Motoyama, H., Noone, D., Oerter, H., Petit, J. R., Royer, A., Uemura, R., Schmidt, G. A., Schlosser, E., Simões, J. C., Steig, E. J., Stenni, B., Stievenard, M., van den Broeke, M. R., van de Wal, R. S., van de Berg, W. J., Vimeux, F., and White, J. W. C.: A review of Antarctic surface snow isotopic composition: Observations, atmospheric circulation, and isotopic modelling, J. Clim., 21, 3359-3387, 2008.

https://doi.org/10.5194/egusphere-2024-4021
Preprint. Discussion started: 9 January 2025

McDowell, N. G., Bond, B. J., Dickman, L. T., Ryan, M. G., and Whitehead, D.: Relationships between tree height and carbon isotope discrimination. In F. C. Meinzer, B. Lachenbruch and T. E. Dawson (Eds). Size-and age-related changes in tree structure and function (pp. 255-286). The Netherlands: Springer Netherlands, 2011.

Meyers, S., Malinverno, A., Hinnov, L., Zeeden, C. and Moron, V.: astrochron: A Computational Tool for Astrochronology, 2019.

Moossen, H., Bendle, J., Seki, O., Quillmann, U., and Kawamura, K.: North Atlantic Holocene climate evolution recorded by high-resolution terrestrial and marine biomarker records, Quat. Sci. Rev., 129, 111-127, 2015.

Naish, T. R., Woolfe, K. J., Barrett, P. J., Wilson, G. S., Atkins, C., Bohaty, S. M., Bücker, C.J., Claps, M., Davey, F.J., Dunbar, G.B., Dunn, A.G., Fielding, C.R., Florindo, F., Hannah, M.J., Harwood, D.M., Henrys, S.A., Krissek, L.A., Lavelle, M., van der Meer, J., McIntosh, W.C., Niessen, F., Passchier, S., Powell, R.D., Roberts, A.P., Sagnotti, L., Scherer, R.P., Strong, C.P., Talarico, F., Verosub, K.L., Villa, G., Watkins, D.K., Webb, P.-N., and Wonik, T.: Orbitally induced oscillations in the East Antarctic ice sheet at the Oligocene/Miocene boundary, Nature, 413, 719-723, 2001.

Pälike, H., Norris, R.D., Herrie, J.O., Wilson, P.A., Coxall, H.K., Lear, C.H., Shackleton, N.J., Tripati, A.K., and Wade, B.S.: The heartbeat of the Oligocene climate system, Science, 314, 1894-1898, 2006.

Pancost, R. D., Baas, M., van Geel, B., and Sinninghe Damsté, J. S.: Biomarkers as proxies for plant inputs to peats: an example from a sub-boreal ombrotrophic bog, Org. Geochem., 33, 675-690, 2002.

Paxman, G. J., Jamieson, S. S., Hochmuth, K., Gohl, K., Bentley, M. J., Leitchenkov, G., and Ferraccioli, F.: Reconstructions of Antarctic topography since the Eocene–Oligocene boundary, Palaeogeogr. Palaeoclimatol. Palaeoecol., 535, 109346, 2019.

Pekar, S. F., and DeConto, R. M.: High-resolution ice-volume estimates for the early Miocene: Evidence for a dynamic ice sheet in Antarctica, Palaeogeogr. Palaeoclimatol. Palaeoecol., 231, 101-109, 2006.

Peri, P. L., Ladd, B., Pepper, D. A., Bonser, S. P., Laffan, S. W., and Amelung, W.: Carbon ($\delta^{13}C$) and nitrogen (δ15 N) stable isotope composition in plant and soil in Southern Patagonia's native forests, Glob. Change Biol., 18, 311-321, 2012.

Polissar, P. J., Freeman, K. H., Rowley, D. B., McInerney, F. A., and Currie, B. S.: Paleoaltimetry of the Tibetan Plateau from D/H ratios of lipid biomarkers, Earth Planet. Sci. Lett., 287, 64-76, 2009.

Polissar, P. J., Rose, C., Uno, K. T., Phelps, S. R., and deMenocal, P.: Synchronous rise of African C4 ecosystems 10 million years ago in the absence of aridification, Nat. Geosci., 12, 657-660, 2019.

Poynter, J. G., Farrimond, P., Robinson, N., and Eglinton, G.: Aeolian-derived higher plant lipids in the marine sedimentary record: Links with palaeoclimate. In M. Leinen and M. Sarnthein (Eds.) Paleoclimatology and paleometeorology: modern and past patterns of global atmospheric transport (pp. 435-462). Springer Netherlands, 1989.

https://doi.org/10.5194/egusphere-2024-4021
Preprint. Discussion started: 9 January 2025

Prebble, J. G., Raine, J. I., Barrett, P. J., and Hannah, M. J.: Vegetation and climate from two Oligocene glacioeustatic sedimentary cycles (31 and 24 Ma) cored by the Cape Roberts Project, Victoria Land Basin, Antarctica, Palaeogeogr. Palaeoclimatol. Palaeoecol., 231, 41-57, 2006.

Read, J., and Farquhar, G.: Comparative studies in Nothofagus (Fagaceae). I. Leaf carbon isotope discrimination, Funct. Ecol., 5, 684-695, 1991.

Read, J., Hill, R. S., and Hope, G. S.: Contrasting responses to water deficits of Nothofagus species from tropical New Guinea and high-latitude temperate forests: can rainfall regimes constrain latitudinal range?, J. Biogeogr., 37(10), 1962-1976, 2010.

Sachse, D., Radke, J., and Gleixner, G.: Hydrogen isotope ratios of recent lacustrine sedimentary n-alkanes record modern climate variability, Geochim. Cosmochim. Acta, 68, 4877-4889, 2004.

Sachse, D., Billault, I., Bowen, G. J., Chikaraishi, Y., Dawson, T. E., Feakins, S. J., Freeman, K. H., Magill, C. R., McInerney, F. A., van der Meer, M. T. J., Polissar, P., Robins, R. J., Sachs, J. P., Schmidt, H. -L., Sessions, A. L., White, J. W. C., West, J. B., & Kahmen, A., Molecular paleohydrology: Interpreting the hydrogen-isotopic composition of lipid biomarkers from photosynthesizing organisms, Annu. Rev. Earth Planet. Sci., 40, 221-249, 2012.

Schefuß, E., Ratmeyer, V., Stuut, J. B. W., Jansen, J. H. F., and Sinninghe Damsté, J. S.: Carbon isotope analyses of n-alkanes in dust from the lower atmosphere over the central eastern Atlantic, Geochim. Cosmochim. Acta, 67, 1757-1767, 2003.

Schlanser, K., Diefendorf, A. F., Greenwood, D. R., Mueller, K. E., West, C. K., Lowe, A. J., Basinger, J. F., Currano, E. D., Flynn, A. G., Fricke, H. C., Geng, J., Meyer, H. W. and Peppe, D. J.: On geologic timescales, plant carbon isotope fractionation responds to precipitation similarly to modern plants and has a small negative correlation with pCO_2, Geochim. Cosmochim. Acta, 270, 264-281, 2020.

Schubert, B. A., and Jahren, A. H.: Global increase in plant carbon isotope fractionation following the Last Glacial Maximum caused by increase in atmospheric pCO_2, Geology, 43, 435-438, 2015.

Sessions, A. L., Burgoyne, T. W., Schimmelmann, A., and Hayes, J. M.: Fractionation of hydrogen isotopes in lipid biosynthesis, Org. Geochem., 30, 1193-1200, 1999.

Shanahan, T. M., Hughen, K. A., Ampel, L., Sauer, P. E., and Fornace, K.: Environmental controls on the $^{2}H/^{1}H$ values of terrestrial leaf waxes in the eastern Canadian Arctic, Geochim. Cosmochim. Acta, 119, 286-301, 2013.

Sturm, M., Schimel, J., Michaelson, G., Welker, J. M., Oberbauer, S. F., Liston, G. E., Fahnestock, J., and Romanovsky, V. E.: Winter biological processes could help convert arctic tundra to shrubland. Bioscience, 55, 17-26, 2005.

Tibbett, E. J., Scher, H. D., Warny, S., Tierney, J. E., Passchier, S., and Feakins, S. J.: Late Eocene record of hydrology and temperature from Prydz Bay, East Antarctica, Paleoceanogr. Paleoclimatol., 36, e2020PA004204, 2021.

https://doi.org/10.5194/egusphere-2024-4021
Preprint. Discussion started: 9 January 2025

Tipple, B. J., and Pagani, M.: The early origins of terrestrial C4 photosynthesis, Annu. Rev. Earth Planet. Sci., 35, 435-461, 2007.

Tipple, B. J., Meyers, S. R., and Pagani, M.: Carbon isotope ratio of Cenozoic CO_2: A comparative evaluation of available geochemical proxies, Paleoceanography, 25, PA3202, doi:10.1029/2009PA001851, 2010.

Vogts, A., Moossen, H., Rommerskirchen, F., and Rullkötter, J.: Distribution patterns and stable carbon isotopic composition of alkanes and alkan-1-ols from plant waxes of African rain forest and savanna C_3 species. Org. Geochem., 40, 1037-1054, 2009.

Warny, S., Askin, R. A., Hannah, M. J., Mohr, B. A., Raine, J. I., Harwood, D. M., Florindo, F., and SMS Science Team.: Palynomorphs from a sediment core reveal a sudden remarkably warm Antarctica during the middle Miocene, Geology, 37, 955-958, 2009.

Wei, L. J., Raine, J. I., and Liu, X. H.: Terrestrial palynomorphs of the Cenozoic Pagodroma Group, northern Prince Charles Mountains, East Antarctica, Antarct. Sci., 26, 69-79, 2014.

Welker, J. M., Jónsdóttir, I. S., and Fahnestock, J. T.: Leaf isotopic (δ 13 C and δ 15 N) and nitrogen contents of Carex plants along the Eurasian Coastal Arctic: results from the Northeast Passage expedition, Polar Biol., 27, 29-37, 2003.

Westerhold, T., Marwan, N., Drury, A. J., Liebrand, D., Agnini, C., Anagnostou, E., Barnet, J. S. K., Bohaty, S. M., De Vleeschouwer, D., Florindo, F., Frederichs, T., Hodell, D. A., Holbourn, A. E., Kroon, D., Lauretano, V., Littler, K., Lourens, L. J., Lyle, M., Pälike, H., Röhl, U., Tian, J., Wilkens, R. H., Wilson, P. A. and Zachos, J. C.: An astronomically dated record of Earth's climate and its predictability over the last 66 million years, Science, 369, 1383-1387, 2020.

Wu, M. S., Feakins, S. J., Martin, R. E., Shenkin, A., Bentley, L. P., Blonder, B., Salinas, N., Asner, G. P. and Malhi, Y.: Altitude effect on leaf wax carbon isotopic composition in humid tropical forests, Geochim. Cosmochim. Acta, 206, 1-17, 2017.

Yang, H., Pagani, M., Briggs, D. E., Equiza, M. A., Jagels, R., Leng, Q., and LePage, B. A.: Carbon and hydrogen isotope fractionation under continuous light: implications for paleoenvironmental interpretations of the High Arctic during Paleogene warming, Oecologia, 160, 461-470, 2009.

Yang, H., Liu, W., Leng, Q., Hren, M. T., and Pagani, M.: Variation in n-alkane δD values from terrestrial plants at high latitude: Implications for paleoclimate reconstruction, Org. Geochem., 42, 283-288, 2011.

Zachos, J. C., Flower, B. P., and Paul, H.: Orbitally paced climate oscillations across the Oligocene/Miocene boundary, Nature, 388, 567-570, 1997.

https://doi.org/10.5194/egusphere-2024-4021
Preprint. Discussion started: 9 January 2025

Zachos, J. C., Shackleton, N. J., Revenaugh, J. S., Pälike, H., and Flower, B. P.: Climate response to orbital forcing across the Oligocene-Miocene boundary, Science, 292, 274-278, 2001.

575 Zhou, W., Xie, S., Meyers, P. A., and Zheng, Y.: Reconstruction of late glacial and Holocene climate evolution in southern China from geolipids and pollen in the Dingnan peat sequence, Org. Geochem., 36, 1272-1284, 2005.